Journal of Sound and Vibration (1997) **206**(4), 507–521

A NEW SYMMETRIC AND POSITIVE DEFINITE BOUNDARY ELEMENT FORMULATION FOR LATERAL VIBRATIONS OF PLATES

G. Davì and A. Milazzo

Dipartimento di Meccanica e Aeronautica, Università di Palermo, Viale delle Scienze 90128 *Palermo, Italy*

(*Received* 4 *March* 1997, *and in final form* 1 *May* 1997)

A new symmetric and positive definite boundary element method in the time domain is presented for the dynamic analysis of thin elastic plates. The governing equations of the problem are obtained from a variational principle in which a hybrid modified functional is employed. The functional is expressed in terms of the domain and boundary basic variables in plate bending, assumed to be independent of each other. In the discretized model the boundary variables are expressed by nodal values, whereas the internal displacement field is modelled by a superposition of static fundamental solutions. The equations of motion are deduced from the functional stationarity conditions and they constitute a linear system of ordinary differential equations expressed in terms of nodal displacements. The structural operators are frequency independent and preserve the symmetry and definiteness properties of the continuum. Moreover these operators are calculated by performing boundary integrations of regular kernels only. Some applications to free vibrations and self-excited vibrations under aerodynamic loads have been worked out to test the accuracy of the proposed method. The numerical results have been found in very good agreement with those obtained by using other solution techniques by which the accuracy of the present boundary element model is demonstrated.

1. INTRODUCTION

The analysis of lateral vibrations of plates is a subject of great importance in engineering practice due to the very diffuse employment of these structural members. The plate dynamic problem has been approached by using both analytical and numerical methods. However, realistic problems of dynamic analysis of thin elastic plates with complicated geometries and boundary conditions can be solved only numerically. The most popular method employed for plate lateral vibration investigation is the finite element method (FEM) [1], which has been applied by many researchers to solve various problems. Recently, the boundary element method (BEM) has been proposed as an accurate and effective technique to approach plate vibrations and dynamic problems in general [2, 3]. According to the first integral formulation for elastodynamics presented by Cruse and Rizzo [4], some authors have developed direct boundary element approaches both in the time domain and in the frequency domain [5–9]. These methods require the use of dynamic fundamental solutions expressed in terms of Hankel functions of complex argument, involving the frequency. As a result of this, the free vibration problem is governed by frequency dependent complex matrices and its solution is therefore based on the computational inefficient zero-determinant searching. To obtain a more efficient and versatile BEM model for plate dynamics, Bezine [10] proposed the employment of static

0022–460X/97/390507 + 15 $25.00/0/sv971093

fundamental solutions. Unfortunately, this approach gives rise to a domain integral related to the inertia forces which affects the pure boundary character of the dynamic model. Many different approaches have been presented in the field of the so-called boundary-domain element method. Tanaka *et al*. [11], Providakis and Beskos [12] and Katsikadelis [13] have presented boundary-domain formulations which require a domain discretization and the evaluation of domain integrals with the consequent increase in the computational effort. Various techniques have been developed in order to recover the pure boundary character of the dynamic model. The most successful and effective approach to overcome the drawback of the domain discretization is the Dual Reciprocity Method proposed by Nardini and Brebbia [14]. The application of the Dual Reciprocity BEM [15–17] leads to a linear system, obtained by using a boundary discretization only, with obvious computational advantages. However, in all of the dynamic models proposed, the properties of symmetry and positive definiteness of the continuum are lost and the discrete structural operators are neither symmetric nor positive definite. The loss of these fundamental properties of the continuum makes less efficient the coupling between domains treated by boundary elements and those treated by finite elements which is the best solution for the modelling of many engineering problems. More recently, some variational formulations of BEM have been developed for both elastostatics and elastodynamics [18–23] with the aim of preserving the above-mentioned operator properties. In this paper, a hybrid variational formulation of BEM for plate dynamics is presented, with particular care devoted to plate lateral vibration problems. The method proposed is based on a formulation previously presented by the authors [21–23], which is extended here to analyze the dynamic behaviour of plates. In the method, the domain variables are approximated by a linear combination of static fundamental solutions, whereas the boundary variables are expressed through nodal parameters. In the present work, due to the use of the Kirchhoff approximate linear plate bending theory, internal nodal parameters other than those related to the boundary discretization are also considered. By so doing, the modelling accuracy and efficiency are improved, fitting the original formulation [22, 23] to the problem. The discrete structural operators are frequency independent, symmetric and positive definite. Moreover, they are calculated by performing integrations of non-singular functions on the boundary only. The resolving system is given by a linear system, expressed in terms of displacements, which does not differ in nature from the matrix equations of a finite element formulation. This allows the employment of standard numerical procedures for the solution and makes more efficient the coupling between domains treated by BEM and those treated by FEM. Some applications are presented to test and validate the accuracy and the efficacy of the method proposed. Classical cases of plate free lateral vibrations are treated together with the typical aeronautical problem of the self-excited oscillations experienced by a plate subjected to a supersonic flow on one of its faces, namely "panel flutter" [24]. The last problem has been investigated by using different techniques [25–30] but, to the authors' knowledge, never treated by BEM.

2. BASIC EQUATIONS

Consider a thin, homogeneous, isotropic and linear elastic plate with Ω its middle surface occupying a region of the x–y plane bounded by the contour Γ. According to the Kirchhoff small deflection theory, the behaviour of the plate is determined once the deflection function w is known. The displacement field is given by

$$u = -z\,\frac{\partial w(x, y, \tau)}{\partial x}, \qquad v = -z\,\frac{\partial w(x, y, \tau)}{\partial y}, \qquad w = w(x, y, \tau), \tag{1–3}$$

where τ is the time. The strain field is

$$\mathbf{e} = \begin{bmatrix} e_{xx} \\ e_{yy} \\ e_{xy} \end{bmatrix} = z\mathbf{D}w = z\boldsymbol{\varepsilon}, \tag{4}$$

where $\boldsymbol{\varepsilon}$ denotes the generalized strain vector and $\mathbf{D}$ is defined as

$$\mathbf{D} = [-\partial^2/\partial x^2 \; -\partial^2/\partial y^2 \; -2\,\partial^2/\partial x\,\partial y]^{\mathrm{T}}. \tag{5}$$

The corresponding generalized stresses are the usual bending and twisting moments per unit lengths, and can be expressed as

$$\boldsymbol{\sigma} = \begin{bmatrix} M_{xx} \\ M_{yy} \\ M_{xy} \end{bmatrix} = \mathbf{E}\boldsymbol{\varepsilon} = \mathbf{E}\mathbf{D}w, \tag{6}$$

where

$$\mathbf{E} = D \begin{bmatrix} 1 & v & 0 \\ v & 1 & 0 \\ 0 & 0 & \dfrac{1-v}{2} \end{bmatrix}, \tag{7}$$

in which D is the flexural rigidity of the plate and v is the Poisson's coefficient. With this notation [1], the dynamic equilibrium equation of the plate can be written as

$$\mathbf{D}^{\mathrm{T}}\mathbf{E}\mathbf{D}w + m\ddot{w} - q = 0, \tag{8}$$

where m is the mass density per unit area, $q = q(x, y, \tau)$ is the applied lateral distributed load per unit area and the overdots indicate time derivatives. Moreover, on the constrained boundary Γ_1 the deflection w must satisfy the prescribed kinematical boundary conditions, which are expressed as

$$\mathbf{u} = \overline{\mathbf{u}} \qquad \text{on } \Gamma_1, \tag{9}$$

where $\mathbf{u}$ is the boundary generalized displacement vector the components of which are the deflection w and the normal slope $-\partial w/\partial n$, whereas the overbar denotes prescribed data. On the free boundary Γ_2 the mechanical boundary conditions need to be satisfied,

$$\mathbf{t} = \overline{\mathbf{t}} \qquad \text{on } \Gamma_2, \tag{10}$$

where the components of the boundary generalized traction vector $\mathbf{t}$ are the equivalent shear force T_{eq} and the normal bending M_n. For a plate with NC corners, the mechanical boundary conditions have to be supplemented by the corner conditions

$$\| M_{nt} \|_i = \| \overline{M}_{nt} \|_i, \qquad i = 1, \ldots, NC_2, \tag{11}$$

where NC_2 is the number of free corner points and $\| M_{nt} \|_i$ denotes the fictitious corner force due to the jump of discontinuity of the twisting moment at the ith corner on Γ_2. The deflection w is also subjected to the initial conditions

$$w(x, y, 0) = \bar{w}(x, y), \qquad \dot{w}(x, y, 0) = \dot{\bar{w}}(x, y). \tag{12, 13}$$

3. VARIATIONAL PRINCIPLE

The boundary model for plate dynamics proposed in this paper is based on a modified variational principle previously presented by the authors [21–23]. Let w be the deflection of the plate in the domain Ω and again let $\tilde{\mathbf{u}}$ and $\tilde{\mathbf{t}}$ be the boundary generalized displacement and traction vectors. The functions w, $\tilde{\mathbf{u}}$ and $\tilde{\mathbf{t}}$ are assumed independent of one another. According to references [21–23] and [31] the modified variational principle states that the functional

$$\Pi = \int_{\Omega} [\tfrac{1}{2}\boldsymbol{\varepsilon}^{\mathrm{T}}\mathbf{E}\boldsymbol{\varepsilon} - w(q - m\ddot{w})]\,\mathrm{d}\Omega - \int_{\Gamma} (\mathbf{u} - \tilde{\mathbf{u}})^{\mathrm{T}}\tilde{\mathbf{t}}\,\mathrm{d}\Gamma - \int_{\Gamma_2} \tilde{\mathbf{u}}^{\mathrm{T}}\bar{\mathbf{t}}\,\mathrm{d}\Gamma$$

$$+ \sum_{i=1}^{\mathrm{NC}} \langle (w - \tilde{w}) \,\|\, \tilde{M}_{nt} \,\|\, \rangle_i + \sum_{i=1}^{NC_2} \langle \tilde{w} \,\|\, \bar{M}_{nt} \,\|\, \rangle_i \tag{14}$$

is made stationary by the solution of the governing equations of plate dynamics. The notations $\|\cdot\|$ and $\langle\cdot\rangle_i$ indicate the corner force and the value of the function at the ith corner point, respectively. The variation of the functional Π with respect to the independent variables, taking into account the kinematical boundary conditions on Γ_1, namely

$$\tilde{\mathbf{u}} = \bar{\mathbf{u}} \qquad \text{on } \Gamma_1, \tag{15}$$

yields, through integration by parts,

$$\partial\Pi = \int_{\Omega} (\mathbf{D}^{\mathrm{T}}\mathbf{E}\mathbf{D}w + m\ddot{w} - q)^{\mathrm{T}}\,\partial w\,\mathrm{d}\Omega - \int_{\Gamma} (\mathbf{u} - \tilde{\mathbf{u}})^{\mathrm{T}}\,\partial\tilde{\mathbf{t}}\,\mathrm{d}\Gamma + \int_{\Gamma} (\mathbf{D}_n w - \tilde{\mathbf{t}})^{\mathrm{T}}\,\partial\mathbf{u}\,\mathrm{d}\Gamma$$

$$- \int_{\Gamma_2} (\bar{\mathbf{t}} - \tilde{\mathbf{t}})^{\mathrm{T}}\,\partial\tilde{\mathbf{u}}\,\mathrm{d}\Gamma - \sum_{i=1}^{NC} \langle (\| M_{nt} \| - \| \tilde{M}_{nt} \|)\,\partial w \rangle_i - \sum_{i=1}^{NC_2} \langle (\| \tilde{M}_{nt} \| - \| \bar{M}_{nt} \|)\,\partial\tilde{w} \rangle_i . \tag{16}$$

In equation (16), $\mathbf{D}_n$ denotes the operator that provides the boundary generalized traction vector $\mathbf{t}$ in terms of the deflection w,

$$\mathbf{t} = \begin{bmatrix} T_{eq} \\ M_n \end{bmatrix} = \mathbf{D}_n w, \tag{17}$$

where

$$\mathbf{D}_n = \begin{bmatrix} -D\left\{\dfrac{\partial}{\partial n}\left(\dfrac{\partial^2}{\partial x^2} + \dfrac{\partial^2}{\partial y^2}\right) + (1 - \upsilon)\,\dfrac{\partial}{\partial s}\dfrac{\partial}{\partial n}\dfrac{\partial}{\partial s}\right\} \\[2ex] -D\left\{\dfrac{\partial^2}{\partial x^2} + \dfrac{\partial^2}{\partial y^2} + (\upsilon - 1)\,\dfrac{\partial^2}{\partial s^2}\right\} \end{bmatrix} \tag{18}$$

and n and s are the normal and tangent directions at the boundary Γ, respectively. The stationarity conditions of equation (16), for arbitrary variations ∂w in Ω, $\partial\tilde{\mathbf{t}}$ on Γ and $\partial\tilde{\mathbf{u}}$ on Γ_2, give the following set of equations:

$$\mathbf{D}^{\mathrm{T}}\mathbf{E}\mathbf{D}w + m\ddot{w} - q = 0 \quad \text{in } \Omega, \tag{19}$$

$$\tilde{\mathbf{u}} = \mathbf{u} \quad \text{on } \Gamma, \qquad \tilde{\mathbf{t}} = \mathbf{t} \quad \text{on } \Gamma, \qquad \tilde{\mathbf{t}} = \bar{\mathbf{t}} \quad \text{on } \Gamma_2, \tag{20–22}$$

$$\| \tilde{M}_{nt} \|_i = \| M_{nt} \|_i, \quad i = 1, \ldots, NC, \qquad \| M_{nt} \|_i = \| \bar{M}_{nt} \|_i, \quad i = 1, \ldots, NC_2. \tag{23, 24}$$

Thus, on the assumption that the compatibility equations (4) and the constitutive equations (6) are satisfied and that the boundary conditions (15) are identically satisfied, the solution of the plate dynamic problem is given in terms of the functions w, $\tilde{\mathbf{u}}$ and $\tilde{\mathbf{t}}$ which make Π stationary.

4. DISCRETIZATION OF THE FUNCTIONAL

In order to obtain a model for the plate dynamic problem by using the variational principle previously described, one can consider the plate boundary discretized by boundary elements. Also, one can consider some additional nodes within the domain Ω other than those introduced by the boundary discretization. The domain displacement field is approximated by means of a linear combination of trial functions w_i^*:

$$w = \sum_i w_i^* s_i \tag{25}$$

The trial functions w_i^* are chosen to be the solutions in an infinite plate corresponding to a generic load q_i^*. Thus these solutions correspond to the solutions of the equation

$$\mathbf{D}^{\mathrm{T}}\mathbf{E}\mathbf{D}w_i^* = q_i^*(x, y) \tag{26}$$

in an infinite domain. The generalized displacements on the boundary Γ can be therefore expressed in terms of trial functions as

$$\mathbf{u} = \begin{bmatrix} w \\ -\partial w/\partial n \end{bmatrix} = \begin{bmatrix} \mathbf{W}^* \\ -\partial \mathbf{W}^*/\partial n \end{bmatrix} \mathbf{s} = \mathbf{U}^*\mathbf{s}, \tag{27}$$

where $\mathbf{s}$ is the vector of the unknown time dependent coefficients s_i and $\mathbf{W}^*$ is the matrix of the trial functions w_i^*. The boundary generalized displacement and traction variables are expressed as

$$\tilde{\mathbf{u}} = \begin{bmatrix} \tilde{w} \\ -\partial \tilde{w}/\partial n \end{bmatrix} = \mathbf{N}\boldsymbol{\delta} = \begin{bmatrix} \mathbf{N}_{w1} & \mathbf{N}_{w2} \\ \mathbf{N}_{\varphi 1} & \mathbf{N}_{\varphi 2} \end{bmatrix} \begin{bmatrix} \boldsymbol{\delta}_1 \\ \boldsymbol{\delta}_2 \end{bmatrix}, \tag{28}$$

$$\tilde{\mathbf{t}} = \begin{bmatrix} \tilde{T}_{eq} \\ \tilde{M}_n \end{bmatrix} = \boldsymbol{\Psi}\mathbf{p}, \tag{29}$$

where $\boldsymbol{\delta}$ and $\mathbf{p}$ are the nodal displacements and tractions, $\mathbf{N}$ and $\boldsymbol{\Psi}$ are matrices of shape functions, and the subscripts 1 and 2 refer to constrained and free nodal displacements respectively. By substituting these approximations for w, $\tilde{\mathbf{u}}$, and $\tilde{\mathbf{t}}$ in equation (14), the expression for the functional Π for the plate is obtained in its discretized form. The stationarity conditions of Π with regard to $\mathbf{s}$, $\boldsymbol{\delta}_2$ and $\mathbf{p}$, after integration by parts, yield

$$\left(\int_\Gamma \mathbf{U}^{*\mathrm{T}}\mathbf{P}^* \, \mathrm{d}\Gamma - \sum_{i=1}^{NC} \langle \mathbf{W}^{*\mathrm{T}} \| \mathbf{M}_{nt}^* \| \rangle_i + \int_\Omega \mathbf{W}^{*\mathrm{T}}\mathbf{Q}^* \, \mathrm{d}\Omega \right) \mathbf{s} + m \int_\Omega \mathbf{W}^{*\mathrm{T}}\mathbf{W}^* \, \mathrm{d}\Omega \, \ddot{\mathbf{s}}$$

$$-\int_{\Omega} \mathbf{W}^{*\mathrm{T}} q \,\mathrm{d}\Omega - \int_{\Gamma} \mathbf{U}^{*\mathrm{T}} \boldsymbol{\Psi} \,\mathrm{d}\Gamma \mathbf{p} + \sum_{i=1}^{NC} \langle \mathbf{W}^{*\mathrm{T}} \| \tilde{M}_{nt} \| \rangle_i = \mathbf{0}, \tag{30}$$

$$\int_{\Gamma} \mathbf{N}_2^{\mathrm{T}} \boldsymbol{\Psi} \,\mathrm{d}\Gamma \mathbf{p} - \int_{\Gamma_2} \mathbf{N}_2^{\mathrm{T}} \bar{\mathbf{t}} \,\mathrm{d}\Gamma + \sum_{i=1}^{NC_2} \langle \mathbf{N}_{w2}^{\mathrm{T}} \| \bar{M}_{nt} \| \rangle_i - \sum_{i=1}^{NC} \langle \mathbf{N}_{w2}^{\mathrm{T}} \| \tilde{M}_{nt} \| \rangle_i = \mathbf{0}, \tag{31}$$

$$\int_{\Gamma} \boldsymbol{\Psi}^{\mathrm{T}} \mathbf{U}^* \,\mathrm{d}\Gamma \mathbf{s} - \int_{\Gamma} \boldsymbol{\Psi}^{\mathrm{T}} \mathbf{N} \,\mathrm{d}\Gamma \boldsymbol{\delta} = \mathbf{0}, \tag{32}$$

where $\mathbf{P}^*$ is the matrix of the generalized boundary tractions associated with the trial functions w_i^*, whereas the vector $\mathbf{Q}^*$ contains the relative loads q_i^*. Equation (32) is satisfied for every choice of $\boldsymbol{\Psi}$ if

$$\mathbf{U}^*\mathbf{s} = \mathbf{N}\boldsymbol{\delta} \quad \text{on } \Gamma. \tag{33}$$

The relations between the unknown parameters $\mathbf{s}$ and the nodal generalized displacements $\boldsymbol{\delta}$ can be established as follows. Evaluating equation (33) at the boundary nodal points, by virtue of the properties of the shape functions, one obtains n relationships between $\mathbf{s}$ and the boundary nodal displacements $\boldsymbol{\delta}_n$, namely,

$$\bar{\mathbf{U}}^*\mathbf{s} = \delta_n, \tag{34}$$

where the elements of matrix $\bar{\mathbf{U}}^*$ are the values of the functional matrix $\mathbf{U}^*$ at the boundary nodes. In a similar way, collocating equation (25) at the internal nodes, m extra relationships can be established:

$$\bar{\mathbf{W}}^*\mathbf{s} = \delta_m. \tag{35}$$

In equation (35) the elements of the matrix $\bar{\mathbf{W}}^*$ are the values of $\mathbf{W}^*$ calculated at the internal nodes and $\boldsymbol{\delta}_m$ is the internal nodal displacement vector. If the number of trial functions is chosen to be equal to the number of nodal displacements, and these functions are regular and linearly independent, then the matrix

$$\boldsymbol{\Lambda} = \begin{bmatrix} \bar{\mathbf{U}}^* \\ \bar{\mathbf{W}}^* \end{bmatrix} \tag{36}$$

is square and regular and possesses an inverse $\boldsymbol{\Phi} = \boldsymbol{\Lambda}^{-1}$. Therefore, from equations (34) and (35) one has

$$\mathbf{s} = \boldsymbol{\Lambda}^{-1} \begin{bmatrix} \boldsymbol{\delta}_n \\ \boldsymbol{\delta}_m \end{bmatrix} = \boldsymbol{\Phi} \begin{bmatrix} \boldsymbol{\delta}_n \\ \boldsymbol{\delta}_m \end{bmatrix} = [\boldsymbol{\Phi}_n \quad \boldsymbol{\Phi}_m] \begin{bmatrix} \boldsymbol{\delta}_n \\ \boldsymbol{\delta}_m \end{bmatrix} = [\boldsymbol{\Phi}_1 \quad \boldsymbol{\Phi}_2] \begin{bmatrix} \boldsymbol{\delta}_1 \\ \boldsymbol{\delta}_2 \end{bmatrix}. \tag{37}$$

Equations (33) and (37) imply the following expression for $\mathbf{N}$ in terms of trial functions;

$$\mathbf{N} = \mathbf{U}^*\boldsymbol{\Lambda}^{-1} = \mathbf{U}^*\boldsymbol{\Phi} = \mathbf{U}^*[\boldsymbol{\Phi}_1 \quad \boldsymbol{\Phi}_2] = \begin{bmatrix} \mathbf{W}^* \\ -\dfrac{\partial \mathbf{W}^*}{\partial n} \end{bmatrix} [\boldsymbol{\Phi}_1 \quad \boldsymbol{\Phi}_2] = \begin{bmatrix} \mathbf{N}_{w1} & \mathbf{N}_{w2} \\ \mathbf{N}_{\varphi 1} & \mathbf{N}_{\varphi 2} \end{bmatrix}. \tag{38}$$

Pre-multiplying equation (30) by $\boldsymbol{\Phi}_2^{\mathrm{T}}$, by using equations (31) and (37), one obtains the plate dynamic model, which can be written as

$$\mathbf{M}\ddot{\boldsymbol{\delta}}_2 + \mathbf{K}\boldsymbol{\delta}_2 = \int_{\Gamma_2} \mathbf{N}_2^{\mathrm{T}}\overline{\mathbf{t}}\,\mathrm{d}\Gamma - \int_{\Omega} \mathbf{N}_{w2}^{\mathrm{T}} q\,\mathrm{d}\Omega - \sum_{k=1}^{NC_2} \langle \mathbf{N}_{w2}^{\mathrm{T}} \,\|\, \overline{M}_{nt} \,\| \rangle_k - \boldsymbol{\Phi}_2^{\mathrm{T}}\mathbf{B}\boldsymbol{\Phi}_1\ddot{\boldsymbol{\delta}}_1 - \boldsymbol{\Phi}_2^{\mathrm{T}}\mathbf{A}\boldsymbol{\Phi}_1\boldsymbol{\delta}_1, \tag{39}$$

where the stiffness matrix $\mathbf{K}$ and the mass matrix $\mathbf{M}$ are given by

$$\mathbf{K} = \boldsymbol{\Phi}_2^{\mathrm{T}}\left(\int_{\Gamma} \mathbf{U}^{*\mathrm{T}}\mathbf{P}^*\,\mathrm{d}\Gamma - \sum_{i=1}^{NC} \langle \mathbf{W}^{*\mathrm{T}} \,\|\, M_{nt}^* \,\| \rangle_i + \int_{\Omega} \mathbf{W}^{*\mathrm{T}}\mathbf{Q}^*\,\mathrm{d}\Omega\right)\boldsymbol{\Phi}_2 = \boldsymbol{\Phi}_2^{\mathrm{T}}\mathbf{A}\boldsymbol{\Phi}_2, \tag{40}$$

$$\mathbf{M} = \boldsymbol{\Phi}_2^{\mathrm{T}} m \int_{\Omega} \mathbf{W}^{*\mathrm{T}}\mathbf{W}^*\,\mathrm{d}\Omega\boldsymbol{\Phi}_2 = \boldsymbol{\Phi}_2^{\mathrm{T}}\mathbf{B}\boldsymbol{\Phi}_2. \tag{41}$$

Notice that the matrices $\mathbf{K}$ and $\mathbf{M}$ are frequency independent, symmetric and positive definite [22, 23]. Therefore, in the approach proposed, these two fundamental properties of the continuum, i.e., symmetry and definiteness of the structural operators, are preserved.

5. BOUNDARY MODEL

In the boundary model based on the proposed formulation, the trial functions w_i^* are chosen to be the static fundamental solutions in an infinite plate corresponding to a point load and a point couple with magnitude c_i^*, applied at the location $\boldsymbol{\zeta}_i$ which is referred as the source point [32]. The fundamental solution due to a point load corresponds to the solution of the equation (26) for a load q_i^* defined as

$$q_i^* = c_i^*\,\delta(\mathbf{x} - \boldsymbol{\zeta}_i) \tag{42}$$

where $\delta(\mathbf{x} - \boldsymbol{\zeta}_i)$ denotes Dirac's function. This fundamental solution is

$$w_i^* = c_i^*\,(r^2/8\pi)\ln r, \tag{43}$$

where r is the distance between the observed point $\mathbf{x}$ and the source point $\boldsymbol{\zeta}_i$. The fundamental solution due to a point couple about an axis orthogonal to the boundary outer normal $\mathbf{n}$ can be directly obtained applying the operator $\partial/\partial n$ to the fundamental solution (43), and it is therefore given by

$$w_i^* = c_i^*\,(r/8\pi)\,(2\ln r + 1)\,\partial r/\partial n. \tag{44}$$

It is worth noting that these fundamental solutions possess the properties requested by the formulation; i.e., they are regular and numerically independent. The trial functions considered, which are associated with the source points, are well suited for computer implementation since they can be directly correlated with the nodal points. According to equation (34), for the boundary nodes where there are two unknown nodal generalized displacements, namely the nodal deflection and normal slope, both the fundamental solutions are defined with the same source point. On the other hand at the internal nodes, as the nodal deflection is the sole unknown, only the fundamental solution due to a point load is considered in accordance with equation (35). For the fundamental solutions carried by the internal nodes the source point is chosen coincident with the node, whereas the source point of the fundamental solutions associated with boundary nodal points is located outside the domain along the boundary outer normal at the node. With this choice of the trial functions, remembering the properties of integrals involving Dirac functions, the domain integral in the stiffness matrix definition, equation (40), can be directly evaluated and the calculation of the stiffness matrix requires only boundary integrations. Moreover, due to the choice of the source points which do not lie on the plate boundary, the kernels involve only non-singular functions with the consequent advantages in computation. The other domain integral that appears in the definition of the mass matrix **M** should require a discretization of the plate domain. To obtain a pure boundary model of the discretized plate, a transformation of this domain integral into boundary integral needs to be performed [22]. Consider the plate loaded by a system of domain forces w_j^*, where w_j^* is the jth fundamental solution. A displacement field φ_j due to this body forces is given by a solution of the equation

$$\mathbf{D}^{\mathrm{T}}\mathbf{E}\mathbf{D}\varphi_j - w_j^* = 0 \quad \text{in } \Omega. \tag{45}$$

By applying the reciprocity theorem to the solution φ_j due to the body forces w_j^* and to the fundamental solution w_i^*, the generic element B_{ij} of the matrix **B** can be expressed as

$$B_{ij} = m \int_{\Omega} w_i^* w_j^* \,\mathrm{d}\Omega = m \int_{\Omega} w_i^* \mathbf{D}^{\mathrm{T}}\mathbf{E}\mathbf{D}\varphi_j \,\mathrm{d}\Omega = mD \int_{\Gamma} \left\{ w_i^* \frac{\partial}{\partial n}(\nabla^2 \varphi_j) + \nabla^2 w_i^* \frac{\partial \varphi_j}{\partial n} \right.$$

$$\left. - \varphi_j \frac{\partial}{\partial n}(\nabla^2 w_i^*) - \nabla^2 \varphi_j \frac{\partial w_i^*}{\partial n} \right\} \mathrm{d}\Gamma + mc_i^* \int_{\Omega} \varphi_j \delta(\mathbf{x} - \boldsymbol{\zeta}_i) \,\mathrm{d}\Omega. \tag{46}$$

Equation (46), taking again the Dirac's function properties into account, allows one to express the mass matrix in terms of boundary integrals. The expressions for the auxiliary functions φ_j associated with the fundamental solutions, equations (43) and (44), are obtained by integrating analytically equation (45). They are given, respectively, by

$$\varphi_j = c_j^* (r^6/4068\pi)(\ln r - \tfrac{5}{6}), \qquad \varphi_j = c_j^* (r^5/1152\pi)(\tfrac{3}{2}\ln r - 1)\,\partial r/\partial n, \tag{47, 48}$$

By performing the above-described transformation both the mass matrix and the stiffness matrix can be calculated through integration of regular kernels on the boundary only, thus recovering the pure boundary character of the formulation. The dynamic model obtained is constituted of a set of linear differential equations that exhibits the same nature of the most common finite element dynamic resolving systems. Therefore, for the numerical solution, the present Displacement Boundary Method (DBM) allows the application of the standard procedures available for FEM models coupled with the BEM computational advantages.

6. APPLICATIONS AND NUMERICAL RESULTS

Solutions of some problems of plate lateral vibrations are presented here in order to show the accuracy and the efficacy of the proposed method on the basis of which a new computer code has been developed. The applications performed deal with the classical case of the free vibrations of rectangular plates and the so-called panel flutter; i.e., the self-excited oscillations of plates under non-conservative aerodynamic loads. The structural operators are computed through Gaussian quadrature, performing boundary integrations only in accordance with the expressions given in equations (40), (41) and (46). The regular kernels associated with the boundary nodes have been obtained by locating the fundamental solution source point outside the domain along the outward directed normal at the nodal point. The solutions presented are relative to a ratio between the point from the nodal point and the element length equal to 1. It is worth noting that this parameter can be varied within a range of 0·5–2·0 without appreciable influence on the solution accuracy as shown in previous papers [21–23]. The kernels associated with the internal nodes, if these are considered, are instead obtained by making the fundamental solution source point coincident with the node. By virtue of the nature of the resolving system obtained, either for the eigenvalue problem relative to the free vibration or for that linked to the panel flutter analysis, classical standard procedures can be employed for the numerical solution.

6.1. FREE VIBRATIONS

For the free vibration analysis, equation (39) reduces to the classical form

$$(\mathbf{K} - \omega^2\mathbf{M})\hat{\boldsymbol{\delta}}_2 = \mathbf{0}, \tag{49}$$

where ω is the natural frequency of the plate. As the matrices **K** and **M** are frequency independent, symmetric and positive definite, the standard power method can be used for eigenvalue searching. The first example presented deals with the free lateral vibrations of a fully simply supported rectangular plate with side ratio $a/b = 2$, where a is the length and b is the width of the plate. A convergence analysis was carried out with and without the use of additional internal points. The criterion for the choice of the additional internal nodes was to locate them at the intersections of the lines which join corresponding boundary nodes of opposite sides. The convergence curves for the first three modes are shown in Figure 1 in terms of the error with respect to the analytical solution. They reveal the fast convergence rate of the method. It is worth noting that the use of internal points improves the modelling accuracy and therefore gives, as expected, a faster convergence rate. This is due to the introduction of additional dynamic degrees of freedom other than those on the boundary which give the means for an adequate description of the deflection w of the plate by trial functions. The second application deals with the study of fully clamped rectangular plates of different side ratios. The criterion for the choice of the internal nodal points was the same as in the previous example. The results obtained are shown in Table 1, where the number of boundary nodes employed for the analysis is given

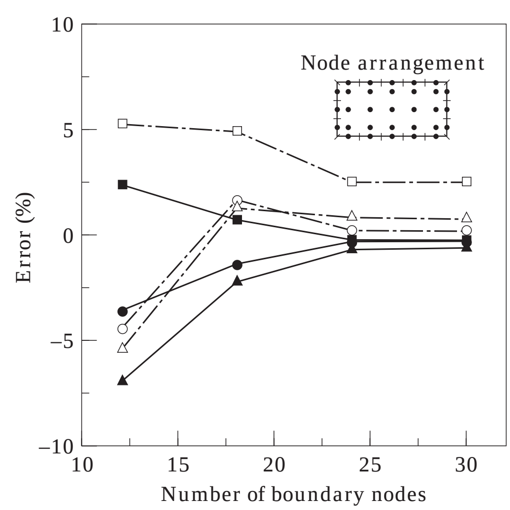

Figure 1. Convergence curves for the simply supported rectangular plate ($a/b = 2$). ●, Mode 1; ▲, mode 2; ■, mode 3, ——, Boundary and internal nodes; — - —, boundary nodes only.

TABLE 1

Natural frequencies for fully clamped rectangular plates

b/a	Boundary nodes	ω_1	ω_2	ω_3	ω_4	ω_5	ω_6
1	40	36·049	73·626	73·626	108·883	132·336	132·336
		(35·984)	(73·408)	(73·408)	(108·200)	(131·920)	(131·920)
		[35·992]	[73·412]	[73·412]	[108·272]	[131·640]	[132·252]
1·25	30	29·999	52·917	69·426	90·861	91·425	129·488
		(29·888)	(52·520)	(68·520)	(89·241)	(89·360)	(124·323)
1·5	30	27·131	42·071	67·157	67·616	81·811	103·972
		(26·994)	(41·720)	(66·124)	(66·528)	(79·800)	(100·800)
2	30	24·723	32·149	45·503	65·010	65·414	73·307
		(24·480)	(31·824)	(44·760)	(63·320)	(64·000)	(71·080)
2·5	30	23·808	28·125	36·054	47·943	64·09	65·177
		(23·520)	(27·808)	(35·404)	(46·680)	(61·480)	(63·08)
3	30	23·361	26·162	31·317	39·164	49·986	63·140
		(23·060)	(25·860)	(30·712)	(38·092)	(47·960)	(60·320)

The values in parentheses are accurate, adapted from reference [33], and the values in square brackets are from reference [34].

and a comparison with the solution of references [33] and [34] is presented. All the results computed are in good agreement with those existing in the literature, whereby the accuracy and the capabilities of the proposed method are demonstrated.

6.2. PANEL FLUTTER

Consider a thin, flat plate with thickness h, length a, width b and mass density ρ. The panel is subjected on one of its faces to a supersonic airstream flowing along direction x with air density ρ_a, flow velocity U_∞ and Mach number M_∞, as shown in Figure 2. Upon assuming that two-dimensional quasi-steady first order piston theory aerodynamics is accurate, the aerodynamic pressure acting on the panel is [35]

$$q = \Delta p = -\frac{\rho_a U_\infty^2}{(M_\infty^2 - 1)^{1/2}} \frac{\partial w}{\partial x} - \frac{\rho_a U_\infty (M_\infty^2 - 2)}{(M_\infty^2 - 1)^{3/2}} \frac{\partial w}{\partial \tau}. \tag{50}$$

By substituting equation (50) into the domain force term of equation (39), and dividing by D/a^3, where D is the plate flexural rigidity, the panel flutter equation is obtained in its classical non-dimensional form [29]:

$$\mathbf{M}\ddot{\boldsymbol{\delta}}_2 + g\mathbf{C}\dot{\boldsymbol{\delta}}_2 + (\mathbf{K} + \lambda \mathbf{K}_A)\boldsymbol{\delta}_2 = \mathbf{0}. \tag{51}$$

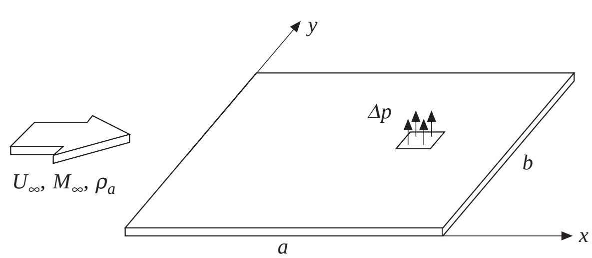

Figure 2. The panel configuration.

In the previous relation, $\mathbf{M}$ and $\mathbf{K}$ are the non-dimensional mass and stiffness matrices, defined in accordance with section 4, whereas

$$\mathbf{C} = \mathbf{\Phi}_2^{\mathrm{T}} \int_\Omega \mathbf{W}^{*\mathrm{T}} \mathbf{W}^* \, \mathrm{d}\Omega \mathbf{\Phi}_2 = \mathbf{M}, \qquad \text{and} \qquad \mathbf{K}_A = \mathbf{\Phi}_2^{\mathrm{T}} \int_\Omega \mathbf{W}^{*\mathrm{T}} \frac{\partial \mathbf{W}^*}{\partial x} \, \mathrm{d}\Omega \mathbf{\Phi}_2 = \mathbf{\Phi}_2^{\mathrm{T}} \mathbf{\Theta} \mathbf{\Phi}_2 \tag{52, 53}$$

model the damping and stiffness aerodynamic operators. The quantities λ and g are defined as

$$\lambda = \rho_a U_\infty^2 a^3 / D(M_\infty^2 - 1)^{1/2}, \qquad g = (M_\infty^2 - 2)\rho_a U_\infty / (M_\infty^2 - 1)^{3/2} \rho h \omega_0, \tag{54, 55}$$

where

$$\omega_0 = \sqrt{D/\rho h a^4}. \tag{56}$$

Like the mass matrix, the aerodynamic stiffness matrix $\mathbf{K}_A$ can also be expressed in terms of boundary integrals, with a consequent improvement in its computation. Indeed, according to the technique described for the transformation of the mass matrix, the domain integral involved in the definition of the generic element Θ_{ij} of the matrix $\mathbf{\Theta}$ can be transformed as follows:

$$\Theta_{ij} = \int_\Omega w_i^* \frac{\partial w_j^*}{\partial x} \, \mathrm{d}\Omega = \int_\Omega w_i^* \left(\mathbf{D}^{\mathrm{T}} \mathbf{E} \mathbf{D} \frac{\partial \varphi_j}{\partial x} \right) \mathrm{d}\Omega = D \int_\Gamma \left\{ w_i^* \frac{\partial}{\partial n} \left(\nabla^2 \left(\frac{\partial \varphi_j}{\partial x} \right) \right) + \nabla^2 w_i^* \frac{\partial}{\partial n} \left(\frac{\partial \varphi_j}{\partial x} \right) \right.$$

$$\left. - \frac{\partial \varphi_j}{\partial x} \frac{\partial}{\partial n} (\nabla^2 w_i^*) - \nabla^2 \left(\frac{\partial \varphi_j}{\partial x} \right) \frac{\partial w_i^*}{\partial n} \right\} \mathrm{d}\Gamma + c_i^* \int_\Omega \frac{\partial \varphi_j}{\partial x} \delta(\mathbf{x} - \boldsymbol{\zeta}_i) \, \mathrm{d}\Omega. \tag{57}$$

With the displacements assumed to be exponential functions of time the solution of equation (51) is sought in the form

$$\boldsymbol{\delta}_2 = \hat{\boldsymbol{\delta}}_2 \, \mathrm{e}^{\alpha\tau}, \tag{58}$$

where, in general, $\alpha = \xi + \mathrm{j}\omega$ is a complex number. Under this assumption, by simple algebraic manipulations [29], equation (51) provides the following eigenvalue problem governing the panel flutter problem:

$$(\mathbf{K} + \lambda \mathbf{K}_A - k\mathbf{M})\hat{\boldsymbol{\delta}}_2 = \mathbf{0}. \tag{59}$$

Here

$$k = -(\alpha/\omega_0)^2 - g \frac{\alpha}{\omega_0} = k_1 + \mathrm{j}k_R \tag{60}$$

The matrices $\mathbf{K}$ and $\mathbf{M}$ are symmetric and positive definite, whereas the master aerodynamic matrix $\mathbf{K}_A$ is non-symmetric. Hence non-real eigenvalues k are expected for $\lambda > 0$. For $\lambda = 0$, the classical free vibration case is recovered, and the eigenvalues are all real and positive. As λ is increased from zero, two of these eigenvalues will usually approach each other and coalesce to $\lambda = \lambda_{coal}$ and become complex conjugate pairs for $\lambda > \lambda_{coal}$, giving rise to self-excited lateral vibrations. This instability occurs at the value $\lambda = \lambda_{cr}$, for which the following condition is satisfied [29]:

$$g = k_I / \sqrt{k_R}. \tag{61}$$

Table 2

Coalescence results for two sides simply supported panel

Number of elements	λ_{coal}	k_{coal}
12	339·575	1039·2
16	343·234	1051·6
20	343·365	1051·9
Exact (reference [29])	343·356	1051·8

The flutter boundary, i.e., the value of λ at which flutter appears, is therefore obtained by solving the eigenvalue problem of equation (59) for different values of the dynamic pressure λ and searching for the condition (61). The most popular case of a panel simply supported along two opposite sides was analyzed and the results compared with those already available in the literature. The results obtained are shown in Table 2 for different discretization schemes in order to test the method convergence rate for this kind of problem. For this analysis no internal points were used because, by virtue of the boundary conditions, the number of boundary degrees of freedom is sufficient to model adequately the lateral displacement w of the plate. The comparison of the coalescence dynamic pressure λ_{coal} and the relative first two coalesced eigenvalues $k_1 = k_2 = k_{coal}$ with the exact values proves that an excellent approximation is obtained employing only a small number of boundary nodes. The variation of the eigenvalues with the dynamic pressure for the panel discretized by using only 20 boundary nodes is shown in Figure 3. The eigenvalues k_1 and k_2 coalesce at $\lambda_{coal} = 343{\cdot}36$, which is the critical dynamic pressure λ_{cr} for linear flutter with no aerodynamic damping ($g = 0$). If some damping is present panel flutter occurs at a value higher than the coalescence dynamic pressure as shown in Figure 4, where the typical response parameters, namely the modal damping parameter ξ and the pulsation ω, are plotted against λ for two different values of the aerodynamic damping g. A comparison of the present results with those obtained by other authors is shown in Figure 5. The panel flutter analysis was also performed for a fully simply supported panel

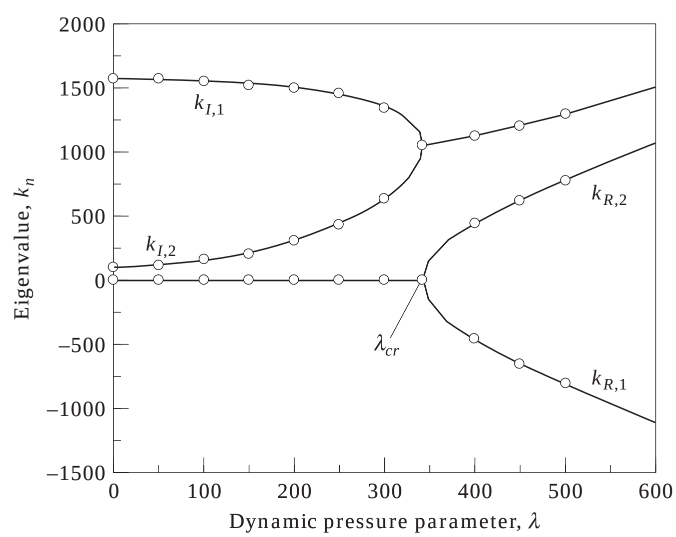

Figure 3. Variation of the eigenvalues with dynamic pressure for the two sides simply supported panel. ——, Present; ○, Mei [29].

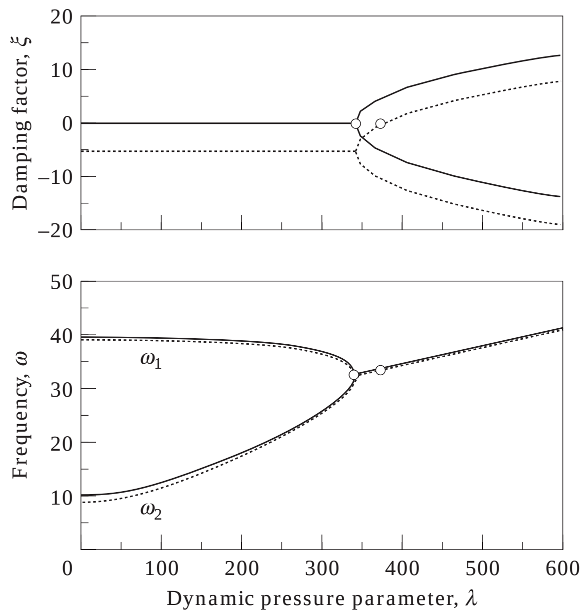

Figure 4. A typical plot of response parameters ξ and ω against dynamic pressure, ○, Flutter condition, ——, $g = 0$; · · · · , $g = 10$.

with side ratio $a/b = 2$. Owing to the symmetry of the aerodynamic forces about the centreline of the plate along the flow direction, only half of the plate was used in the analysis. By so doing, no internal nodes were needed and the desired accuracy was obtained employing 20 boundary nodes only. For this example, the value of the critical dynamic pressure is $\lambda_{cr} = 1091{\cdot}2$, which compares well with the results available in the literature, as shown in Table 3. The results presented prove the accuracy and the effectiveness of the proposed method, also for the investigation of dynamic instability problems.

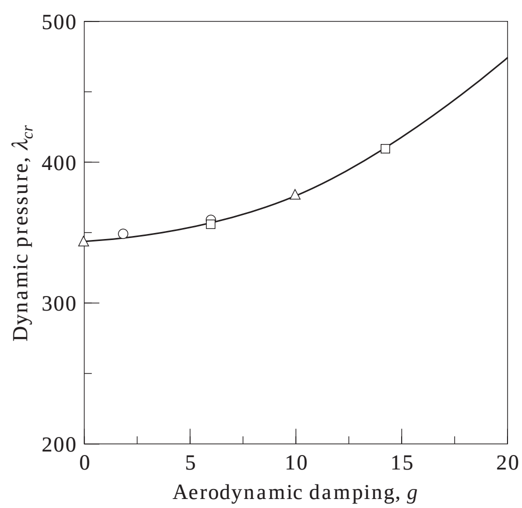

Figure 5. Critical dynamic pressure versus aerodynamic damping. ——, Present; ○, Dowell [26]; □, Kuo *et al*. [28]; △, Sarma and Varadan [30].

TABLE 3

Coalescence results for fully simply supported panel ($a/b = 2$)

	$\lambda_{coal} = \lambda_{cr}$
Present	1091·20
Dugundji [25]	1093·24
Kariappa *et al*. (Ref. 27)	1110·46

7. CONCLUSIONS

A new Displacement Boundary Method (DBM) in the time domain for plate lateral vibration analysis has been presented. The formulation, which is based on a modified variational principle, gives a resolving system that involves nodal displacements. The stiffness and the mass matrices of the boundary discretized body are frequency independent, symmetric and positive definite. They are evaluated by performing boundary integrations only and no integrations of singular kernels are required. Due to the symmetry and definiteness of structural operators, the resolving system exhibits the same properties as the more popular FEM resolving systems, thus allowing the application of standard numerical procedures for the solution, coupled with the computational advantages of BEM. Free vibration analysis of rectangular plates has been carried out, and in this case the search for the natural frequencies comes down to the solution of a classic algebraic eigenvalue problem. Self-excited lateral vibrations induced by non-conservative aerodynamic loads have also been considered to test the ability of the formulation of treating with dynamic instability problems. The results obtained for free and self-excited vibrations are in good agreement with the solutions available in the literature. The new method described here is shown to be very efficient and accurate. The role played by the use of internal nodal points is pointed out. In fact, they are used only when the number of boundary degrees of freedom is inadequate to model the plate internal behaviour through trial functions, or when the higher modes of vibration need to be computed with particular accuracy. The good results obtained suggest the possible application of the method proposed to the solution of many plate dynamic problems, with meaningful computational advantages with respect to the more common field methods.

REFERENCES

1. O. C. ZIENKIEWICZ 1977 *The Finite Element Method*. New York: McGraw-Hill.
2. D. E. BESKOS 1987 *Applied Mechanics Reviews* **40**, 1–23. Boundary element methods in dynamic analysis.
3. D. E. BESKOS 1997 *Applied Mechanics Reviews* **50**, 149–197. Boundary element methods in dynamic analysis: Part II (1986–1996).
4. T. A. CRUSE and F. J. RIZZO 1968 *Journal of Mathematical Analysis and Application* **22**, 244–259. A direct formulation and numerical solution of the general transient elastodynamic problem.
5. J. DOMINGUEZ and E. ALARCON 1981 in *Progress in Boundary Element Methods*, Vol. 1. London: Pentech Press. See chapter 7, Elastodynamics.
6. G. K. K. WONG and J. R. HUTCHINSON 1981 *Boundary Element Methods*. Berlin: Springer-Verlag. See pp. 272–289: An improved boundary element method for plate vibration.
7. Y. NIWA, S. KOBAYASHI and M. KITAHARA 1982 in *Developments in Boundary Element Methods*—2 (P. K. Banerjee and R. P. Shaw, editors), 143–176. Determination of eigenvalues by boundary element method.
8. M. KIHATARA 1985 *Boundary Integral Equation Methods in Eigenvalue Problems of Elastodynamics and Thin Plates*. Amsterdam: Elsevier.
9. R. GALLEGO and J. DOMINGUEZ 1994 *Boundary Element Communications* **5**, 171–180. A two

dimensional boundary element code for time domain formulations using quadratic elements, II: transient elastodynamic problems.
10. G. BEZINE 1980 *Mechanics Research Communications* **7**, 141–150. A mixed boundary integral finite element approach to plate vibration problems.
11. M. TANAKA, K. YAMAGIWA, K. MIYAZAKY and T. UEDA 1988 *Engineering Analysis with Boundary Elements* **5**, 182–188. Free vibration analysis of elastic plate structures by boundary element method.
12. C. P. PROVIDAKIS and D. E. BESKOS 1989 *International Journal for Numerical Methods in Engineering* **28**, 1977–1994. Free and forced vibrations of plates by boundary and interior elements.
13. T. KATSIKADELIS 1990 *Journal of Sound and Vibration* **141**, 313–322. A boundary element solution to the vibration problem of plates.
14. D. NARDINI and C. A. BREBBIA 1982 *Proceedings of the 4th International Seminar on BEM, Southampton*, 312–326. A new approach to free vibration analysis using boundary elements.
15. D. NARDINI and C. A. BREBBIA 1985 in *Topics in Boundary Element Research*, Berlin: Springer-Verlag. See chapter 7: Boundary integral formulation of mass matrices for dynamics analysis.
16. P. W. PARTRIDGE and C. A. BREBBIA 1991 *The Dual Reciprocity Boundary Element Method*. Southampton: Computational Mechanics Publications.
17. J. AGNANTIARIS, D. POLYZOS and D. E. BESKOS 1995 *Proceedings of the IABEM 95 Conference, Hawaii*, 2890–2896. Some studies on dual reciprocity BEM for elastodynamic analysis.
18. N. A. DUMONT 1987 *Proceedings of the 9th International Conference on BEM, Southampton*, 1117–1130. The hybrid boundary element method.
19. T. G. B. DE FIGUEREDO and C. A. BREBBIA 1989 *Proceedings of the 11th International Conference on BEM, Cambridge, U.S.A.*, 47–57. A new hybrid displacement variational formulation of BEM for elastostatics.
20. C. POLIZZOTTO 1991 *Engineering Analysis with Boundary Elements* **8**, 89–93. A boundary min–max principle as a tool for boundary element formulations.
21. G. DAVÌ 1992 *Engineering Analysis with Boundary Elements* **10**, 219–224. A hybrid displacement variational formulation of BEM for elastostatics.
22. G. DAVÌ and A. MILAZZO 1994 *Proceedings of the 16th International Conference on BEM, Southampton*, 505–512. A hybrid displacement variational formulation of BEM for elastodynamics.
23. G. DAVÌ and A. MILAZZO 1994 *Engineering Analysis with Boundary Elements* **14**, 343–348. A symmetric and positive definite variational BEM for 2-D free vibration analysis.
24. E. H. DOWELL 1970 *American Institute of Aeronautics and Astronautics Journal* **8**, 385–399. Panel flutter: a review of the aeroelastic stability of plates and shells.
25. J. DUGUNDJI 1966 *American Institute of Aeronautics and Astronautics Journal* **4**, 1257–1266. Theoretical considerations of panel flutter at high supersonic Mach numbers.
26. E. H. DOWELL 1966 *American Institute of Aeronautics and Astronautics Journal* **4**, 1267–1275. Nonlinear oscillations of a fluttering plate.
27. B. R. S. KARIAPPA 1969 *American Institute of Aeronautics and Astronautics Journal* **7**, 50–54. Application of matrix displacement methods in the study of panel flutter.
28. C. C. KUO, L. MORINO and J. DUGUNDJI 1972 *American Institute of Aeronautics and Astronautics Journal* **10**, 1479–1484. Perturbation and harmonic balance methods for nonlinear panel flutter.
29. C. MEI 1977 *American Institute of Aeronautics and Astronautics Journal* **15**, 1107–1110. A finite-element approach for nonlinear panel flutter.
30. B. S. SARMA and K. VARADAN 1988 *American Institute of Aeronautics and Astronautics Journal* **26**, 566–574. Nonlinear panel flutter by finite-element method.
31. K. WASHIZU 1968 *Variational Methods in Elasticity and Plasticity*. Oxford: Pergamon Press.
32. P. K. BANERJEE and R. BUTTERFIELD 1981 *Boundary Element Methods in Engineering Science*. New York: McGraw-Hill.
33. D. J. GORMAN 1982 *Free Vibration Analysis of Rectangular Plates*. New York: Elsevier/North-Holland.
34. D. YOUNG 1950 *Journal of Applied Mechanics* **17**, 448–452. Vibration of rectangular plates by the Ritz method.
35. H. ASHLEY and G. ZARTARIAN 1956 *Journal of the Aeronautical Sciences* **23**, 1109–1118. Piston theory—a new aerodynamic tool for the aeroelastician.